Circular and helicoidal standing-wave-induced Fréedericksz transition in nematic liquid crystals

E. Brasselet, T. V. Galstyan,* and A. A. Yesayan
Center for Optics, Photonics and Laser, Physics Department, Laval University, Pav. A.-Vachon, Cité Universitaire, Québec, Canada G1K 7P4
(Received 30 March 1998)

We show that the character of the Fréedericksz transition is significantly changed when circular and helicoidal standing electromagnetic fields are used for excitation. Optical control, such as selective enhancement or suppression, of the collective molecular reorientation modes above the transition threshold is achieved. The particular self-modulation of the azimuthal symmetry and angular momentum of the excitation light allow this control. A corresponding theoretical model is proposed and an analytical solution is found, which describes very well the main features observed in the experiment. [S1063-651X(98)09910-3]

PACS number(s): 64.70.Md, 42.70.Df

I. INTRODUCTION

The observation of the light-induced Fréedericksz transition (LIFT) in nematic liquid crystals (NLC) demonstrated the high efficiency of the dielectric torque that may be exerted by light on matter [1]. The nature of the LIFT has been proven to be much richer compared to the magnetic-field-induced Fréedericksz transition (FT) [1–3]. An important advantage of the LIFT is the possibility to control (e.g., selectively enhance or suppress) the modes of the transition by the proper choice of the excitation light intensity and polarization state distribution. For instance, the linearly polarized light-induced FT has been experimentally proven to be a second-order phase transition [1–5]. The use of a circularly polarized traveling (CPT) light reveals hysteresis behavior, changing the character of the transition from second to first order [4]. The dynamics of the LIFT also appears to be changed. Persistent precessions of the NLC director **n** (unit vector showing the average orientation of molecular axes) have been detected near the LIFT threshold, due to the angular momentum transfer from the CPT light to the NLC [6]. The role of the light polarization state in the above-described phenomena has been intensively studied [1–6]. The variation of the light angular momentum and its transfer to the NLC has been used to optically control the director's precession rate, under the condition of conservation of the light's azimuthal symmetry [7,8].

We present in this work the observation of circular and helicoidal standing-electromagnetic-wave induced FT in NLC. We show that the use of these standing waves changes dramatically the character of the FT as far as the kinetics and the steady-state excitation modal behavior of the transition are concerned. Experimental study of these phenomena in the weak perturbation regime confirms our theoretical predictions obtained by analytical solution. Optical control of the behavior of the transition modes is demonstrated.

II. THEORY

The general theoretical background of the LIFT is provided in Ref. [8], where the interaction of *noncoherent copropagating* beams with NLC is detailed as a particular case. We shall discuss hereafter only the theoretical part, which corresponds to the interaction of two *coherent counterpropagating* beams with a NLC, while the same general theoretical background may be used in these two cases.

Let us consider an infinite layer of a homeotropically aligned (director is perpendicular to the cell walls) NLC of thickness L. The director **n** will be described by the polar angles θ and φ, where θ is the tilt angle between **n** and the **z** axis, and φ is the azimuthal angle between the local (n,z) and (x,z) planes (inset of Fig. 1). Consider the case when two circularly polarized counterpropagating (along the z axis) harmonic plane waves, with frequency ω and wave number $k_0=\omega/c$, are normally incident on the NLC:

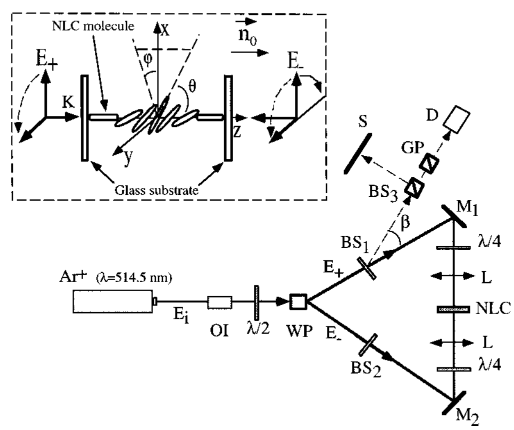

FIG. 1. Experimental setup. E_i: linearly polarized argon ion laser (Ar^+) beam; OI: optical isolator: λ/2: half-wave plate; WP: Wollaston prism; $\vec{E}_+$ and $\vec{E}_-$: optical arms; BS_1, BS_2, and BS_3: beam splitters; M_1 and M_2: mirrors; λ/4: quarter-wave plates; L: lenses (with focal length $f=10.5$ cm); NLC: homeotropic cell of $E7$ nematic (thickness $d=80$ μm); GP: Glann prism; D: detector; S: screen. Inset: Geometry of standing-wave interaction with a homeotropic cell of NLC. $\vec{n}_0$: initial (nonperturbed) director; θ and φ: director polar and azimuthal reorientation angles, respectively, $\vec{E}_+$ and $\vec{E}_-$: counterpropagating fields; K: wave vector of the $\vec{E}_+$ wave; x, y, z: coordinate system.

*Author to whom correspondence should be addressed. FAX: (418) 656-2623. Electronic address: galstian@phy.ulaval.ca

$$\mathbf{E}_+ = E_+ \frac{i\mathbf{l}_\parallel(0) + \mathbf{l}_\perp(0)}{\sqrt{2}} e^{ik_0 z - i\omega t},$$
$$\mathbf{E}_- = E_- \frac{\sigma i\mathbf{l}_\parallel(L) + \mathbf{l}_\perp(L)}{\sqrt{2}} e^{-ik_0 z - i\omega t}, \tag{1}$$

where $\mathbf{l}_\parallel(z) = (-\sin\varphi(z), \cos\varphi(z))$, $\mathbf{l}_\perp(z) = (\cos\varphi(z), \sin\varphi(z))$, $\mathbf{l}_\parallel$ and $\mathbf{l}_\perp$ are unit vectors in the (x,y) plane. The $\mathbf{l}_\parallel$ is parallel to the transverse [in the (x,y) plane] vector component of the director, while the $\mathbf{l}_\perp$ is perpendicular to it. The $\sigma = \pm 1$ defines the form of the total field $\mathbf{E} = \mathbf{E}_+ + \mathbf{E}_-$, as *helicoidal standing wave* (HSW) when $\sigma = -1$, and as *circular standing wave* (CSW) when $\sigma = 1$ [9]. The intensity of the HSW is uniform in space, while it has an electric field, which spatially rotates around the $\mathbf{z}$ axis, like a helix. The total angular momentum of the HSW is vanishing since we have a subtraction of the angular momentums of the counterpropagating CPT waves.

In contrast to the previous case, the electric field of the CSW ($\sigma = 1$) is rotating with optical frequency in each (x,y) plane, as in the case of a CPT wave (see below). Its angular momentum is the sum of the angular momentums of the counterpropagating CPT waves. Another important difference between the two configurations is the spatial distribution of the light intensity. The CSW has a nonuniform intensity distribution along the $\mathbf{z}$ axis. Thus, this distribution would lead to corresponding modulation of the dielectric torque locally exerted by the CSW on NLC. In contrast, the dielectric torque of the HSW has constant absolute (but not uniform) value. Indeed, different NLC domains ''see'' a helicoidally rotating dielectric torque exerted by the HSW. While in the CSW field, the NLC domains placed in the minimums of the light intensity will receive the same elastic torque from the neighboring domains, which are in the intensity maximums of the CSW. This would force these domains to follow the neighboring domains, particularly when taking into account the fact that NLC materials may transfer torques on distances much larger than the period of the intensity modulation [3].

Hereafter, we shall describe quantitatively the interaction of these standing waves with the NLC. We consider a general form of the NLC director excitation, as $\mathbf{n} = n_x\mathbf{e}_x + n_y\mathbf{e}_y + n_z\mathbf{e}_z$, where $n_x = \sin\theta\cos\varphi$, $n_y = \sin\theta\sin\varphi$, $n_z = \cos\theta$.

We assume that all functions depend upon z only using the plane-wave approximation. Additionally, we look for the spatial and temporal behavior of the azimuthal angle φ as

$$\varphi(z,t) = \Omega t + \alpha(z), \tag{2}$$

where $\alpha(z)$ represents the director deformation twisting and Ω is the rotation rate around the z axis of a given director configuration.

In order to find the established configuration of the director above the LIFT threshold, it is necessary, first of all, to take into account the perturbations θ and φ in solution of Maxwell's equations in the NLC. We find these solutions (describing the waves propagating in the medium), using the geometrical optics approximation [2,8], for the ordinary and extraordinary wave components (associated with E_+) as

$$\mathbf{E}_{+,o} = iA_+(-\sin\varphi, \cos\varphi, 0)\exp(ik_0\sqrt{\varepsilon_\perp}z),$$
$$\mathbf{E}_{+,e} = (\varepsilon_{zz}/\varepsilon_\parallel)^{1/4}A_+(\cos\varphi, \sin\varphi, -\varepsilon_a\sin 2\theta/(2\varepsilon_{zz})) \tag{3}$$
$$\times\exp\left(ik_0\int_0^z\sqrt{\varepsilon_\perp\varepsilon_\parallel/\varepsilon_{zz}}dz'\right),$$

and for the waves associated with E_- wave as

$$\mathbf{E}_{-,o} = \sigma iA_-(-\sin\varphi, \cos\varphi, 0)\exp[ik_0\sqrt{\varepsilon_\perp}(L-z)],$$
$$\mathbf{E}_{-,e} = (\varepsilon_{zz}/\varepsilon_\parallel)^{1/4}A_-(\cos\varphi, \sin\varphi, -\varepsilon_a\sin 2\theta/(2\varepsilon_{zz}))$$
$$\times\exp\left(ik_0\int_z^L\sqrt{\varepsilon_\perp\varepsilon_\parallel/\varepsilon_{zz}}dz'\right),$$

where $A_{+,-} = \tau E_{+,-}/\sqrt{2}$, $\tau = 2/(1+\sqrt{\varepsilon_\perp})$, $P_i/2 = P_{i,o} = P_{i,e} = c\sqrt{\varepsilon_\perp}|A_i|^2/(8\pi)$, $i = +,-$, and dielectric susceptibility tensor of the NLC at the light frequency may be presented as $\varepsilon_{ij} = \varepsilon_\perp\delta_{ij} + \varepsilon_a n_i n_j$, with $\varepsilon_a = \varepsilon_\parallel - \varepsilon_\perp$ [2,3]. The $P_{i,e}$ (or the $P_{i,o}$) represents the ''e'' (respectively, the ''o'') component of the Pointing vector of the ''i'' incident field in the medium, etc.

Using the solutions (3) and the standard variational principle, according to which the free energy density of the light-NLC system has minimal value in the equilibrium state [2,8], one can obtain the final equations for θ and φ. We use the following boundary conditions for θ and φ to supplement this problem [4]:

$$\theta(z=0) = \theta(z=L) = 0$$

and (4)

$$d\alpha/dz(z=0) = d\alpha/dz(z=L) = 0.$$

We will further seek the polar perturbation in the following form:

$$\theta(z) = \theta_0\sin qz, \quad q = \pi/L, \tag{5}$$

and we will assume a weak perturbation regime:

$$\Delta = k_0\sqrt{\varepsilon_\perp}\int_0^L\sqrt{\varepsilon_\parallel/\varepsilon_{zz}}dz' - k_0\sqrt{\varepsilon_\perp}z$$
$$= k_0\sqrt{\varepsilon_\perp}L\theta_0^2\varepsilon_a/(4\varepsilon_\parallel) \ll 1, \tag{6}$$

which supposes a small nonlinear phase shift between extraordinary and ordinary waves, as in Ref. [8]. The obtained final form for the φ perturbation is

$$\Omega = \frac{\Delta}{2}\frac{1+\sigma R}{1+R}\frac{K_3 q^2}{\gamma},$$
$$\alpha(z) = \frac{\Delta}{4}\frac{1-\sigma R}{1+R}f\left(\frac{z}{L}\right), \tag{7}$$

where $f(\xi) = 1 - (1/2)[\xi + \sin(2\pi\xi)/(2\pi)] - \pi\xi(1-\xi)\cot(\pi\xi)$, $R \equiv |A_+|^2/|A_-|^2$, K_i is Frank's elastic constants, and γ is the orientational viscosity of the NLC.

Following Ref. [8], we will find the polar perturbation amplitude θ_0:

$$\theta_0^2 = \frac{(|A_+|^2 + |A_-|^2)/I_{\text{lin}} - 1}{(4\varepsilon_\perp - 5\varepsilon_a)/(8\varepsilon_\parallel) - (K_3 - K_1)/(2K_3)}, \quad (8)$$

where $I_{\text{lin}} = 8\pi\varepsilon_\parallel K_3 q^2/(\varepsilon_a \varepsilon_\perp)$.

These solutions demonstrate important characteristics of the LIFT, when using CSW and HSW. First, the director's polar perturbation threshold corresponds to the total Poynting vector value:

$$P_{\text{tot}} = \sum_{i=1}^{2} (P_{i,o} + P_{i,e}) = I_{\text{tot}} c \sqrt{\varepsilon_\perp}/(8\pi) = 2P_{\text{lin}}, \quad (9)$$

which is obtained by requiring $I_{\text{tot}} = 2(|A_+|^2 + |A_-|^2) \geqslant 2I_{\text{lin}} = I_{\text{th}}$. Thus, the LIFT threshold for both CSW and HSW does not depend upon σ and is the same as in the single CPT wave case, which is twice the linear polarized light-induced transition threshold [2,8].

Second, the configuration of the director depends quite differently upon parameters I_{tot} and $\delta = |A_+|^2 - |A_-|^2$ for CSW ($\sigma = 1$) and HSW ($\sigma = -1$) cases [see Eq. (7)]. Namely, in the CSW case, the director's azimuthal rotation rate Ω is proportional to I_{tot}, while the director's twist perturbation is proportional to δ. In addition, the direction of the twist is defined also by the sign of δ. In the HSW case, the situation is changed. Thus, in the case of equal intensities of counterpropagating beams (when $\delta = 0$), the director is reoriented in a plane ($\alpha = \text{const}$) that rotates ($\Omega \neq 0$) around the z axis for the CSW case. In contrast, we obtain a nonplanar ($\alpha \neq \text{const}$) but stable ($\Omega = 0$) director reorientation for the HSW case, etc.

III. EXPERIMENTAL RESULTS AND DISCUSSION

A. Experimental setup and interaction geometry

The experimental setup we have used to study the LIFT in the field of CSW and HSW is sketched in Fig. 1. The geometry of the corresponding interaction is represented in the inset of the same figure. The beam E_i of the linearly polarized argon ion laser (operating at 514.5 nm) is traversing an optical isolator (OI) to prevent the destabilization of the laser operation by backpropagating light. The E_i beam is then divided into two separate arms $\vec{E}_+$ and $\vec{E}_-$ by a Wollaston prism (WP). The two obtained beams are made counterpropagating after reflection from mirrors M_1 and M_2. The intensity ratio $R = I_+/I_-$ of these beams is controlled by rotation of the half-wave plate (λ/2), placed between the OI and WP. Quarter-wave plates (λ/4) are placed in the optical paths of both beams to obtain the above-discussed CSW and HSW configurations. The homeotropic cell of NLC $E7$ (from Merck Ltd.) with thickness $d = 80\ \mu$m is placed near to the focal plane of two lenses L (with focal lengths $f = 10.5$ cm) forming a telescope system. The optical path difference of two arms at the NLC film position is negligibly small with respect to the coherence length of the laser. The excitation beams used have Gaussian intensity distribution and their spot diameter at the NLC film is 80 μm. The beam splitter BS_1 (placed at angle $\beta = 1.5°$ with respect to the optical axis) is used to extract a small portion of the counterpropagating beam $\vec{E}_-$ and analyze its polarization state [using a Glann prism (GP) and a detector (D)] and far field intensity distribution (using the reflection from the beam splitter BS_3) at the screen S. The second beam splitter BS_2 makes two arms optically equivalent.

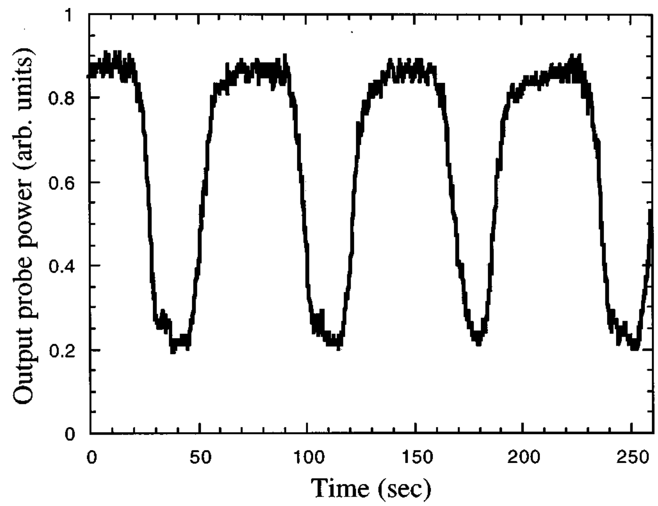

FIG. 2. Demonstration of periodic oscillations of the output beam intensity (detected behind the Glann prism analyzer), resulting from periodic precession of the NLC director under steady-state excitation.

Experiments with standing waves have been carried out as follows. First, we have well adjusted the setup to get two counterpropagating beams that overlap at the NLC film and provide the same LIFT threshold, in the limit of the experimental error (see below). Then, the FT was studied in the field of CSW and HSW, for crossed (e.g., $-45°$ and $+45°$) and parallel ($-45°$ and $-45°$) orientations of two λ/4 plates, respectively.

B. CSW excitation

The LIFT threshold power value in the field of the CSW ($\sigma = 1$) was found to be $P_{\text{CSW}} = 2.2\ \text{kW/cm}^2$, which is slightly higher, but of the same order as for a CPT wave (in the limit of 17% error). The LIFT threshold value for the CPT beam was measured in a separate experiment (to be $P_{\text{CPT}} = 1.9\ \text{kW/cm}^2$), using the same experimental setup and by simply removing one of the counterpropagating beams. The increase of the threshold could be resulting from the nonideal overlapping of two counterpropagating beams, since the detected threshold overcomes the CPT-wave-induced FT threshold. The overlapping problem may be important also due to the comparable sizes (indeed the same) of the beam waist and NLC thickness, which limit the plane-wave approximation we have used in our theoretical analysis. Further study of the modal behavior of the LIFT was carried on in the following manner. The total intensity of the light was adjusted as near as possible (above) to the threshold value and the LIFT was studied in transient and steady-state excitation regimes. Similar to cases reported earlier, director persistent precessions [6–8] were observed (Fig. 2) due to the transfer of the light angular momentum to the NLC. This is in good agreement with our theoretical predictions, corresponding to the case $\delta = 0$ and $\sigma = 1$ [see Eq. (7)]. Variations of δ at fixed I_{tot} (by reorientation of the λ/2, Fig.

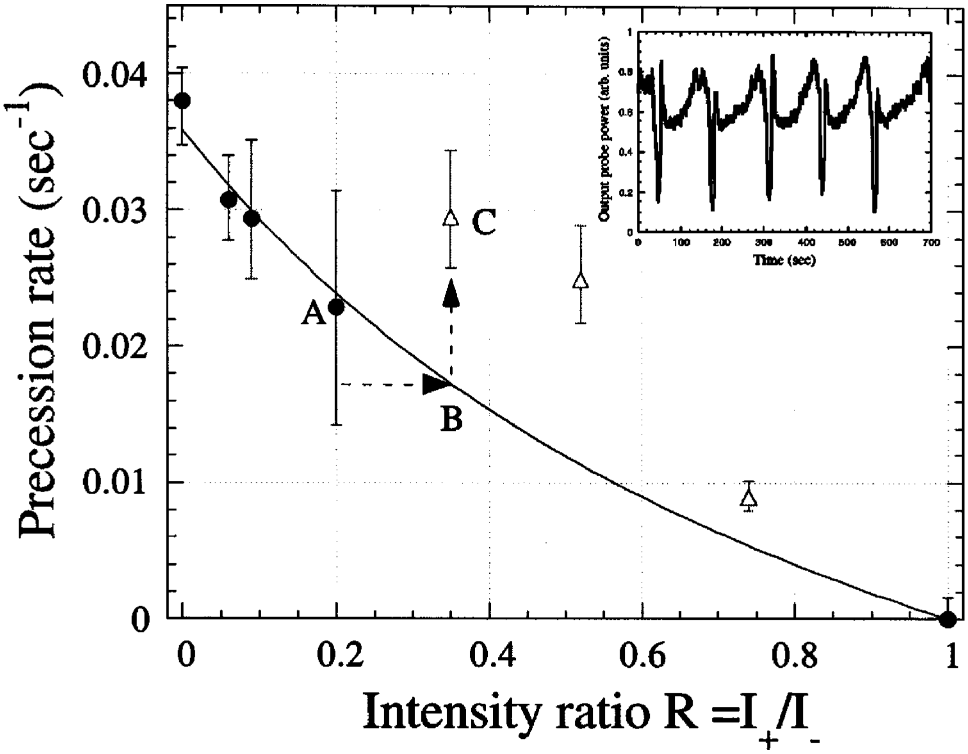

FIG. 3. Demonstration of the director precession control by a helicoidal standing wave. Director precession rate Ω is shown vs the intensity ratio $R=I_+/I_-$ of counterpropagating beams for fixed total intensity $I_{tot}=I_+ + I$ (closed circles) and for growing (with R) total intensity I_{tot} (open triangles). Points A and C correspond to periodic oscillation, while the point B corresponds to the beating regime. The solid line is a theoretical fit using the Eq. (8). Inset: Demonstration of the output beam intensity dynamic modulation in the quasiperiodic beating regime.

1) do not lead to detectable variations of the precession rate. This also agrees well with Eq. (7), since Ω is proportional to I_{tot}, but not to δ.

C. HSW excitation

The FT in the field of the HSW ($\sigma=-1$) was studied in the same manner as in Sec. III B. The LIFT threshold value here was also found to be higher than the CPT-wave-induced FT threshold, within the limit of 20% of the experimental error. Nonideal overlapping could be also responsible for the threshold overcoming. However, more detailed studies are planned to be carried out in the near future to clarify this question [10]. The director's reorientation for near threshold excitation appears to be very stable (for the case $\delta=0$) without dynamic precessions, beatings, etc. This is in excellent agreement with our theoretical predictions [see Eq. (7)]. The breakdown of the condition $\delta=0$ brings to the induction of controllable director precessions. Thus, the variation of δ (or the intensity ratio R) at fixed I_{tot} leads to the continuous change of the director's precession rate (filled circles, Fig. 3). Regular (sinusoidal) oscillations of the output beam intensity (resulting from director precessions) are obtained for large values of δ (i.e., when $R\rightarrow 0$, in Fig. 3). Nevertheless theory predicts a sinusoidal precession regime in any case, while experiment exhibits beatings and quasiperiodic fluctuations when we increase the value of R (see the inset of Fig. 3). These beatings, as well as any dynamic changes, are strongly damped with further increase of R and completely disappear when $R\rightarrow 1$ (Fig. 3). In this case, the output beam is slightly broadened, which confirms the presence of the director polar perturbation ($\theta\neq 0$). The analysis of the output beam shows that there is no dynamic modulation of its polarization state either. Both the beam broadening and its polarization state are quite stable in time for a fixed total intensity. This is in agreement with our theoretical predictions concerning the absence of director precession ($\Omega=0$) and the presence of static perturbation ($\theta\neq 0$) [see Eq. (7)]. Interestingly, the dynamic behavior of the system is easy to control by combined variations of R and total intensity I_{tot}. Indeed, the possibility of a combined control is shown also by our analytical solutions, however, for the periodic precession regime only. In the experiment, the above-mentioned beatings have been transformed back into sinusoidal oscillations by increasing the I_{tot} in parallel with R (Fig. 3). Namely, the system is initially established in a periodic oscillation regime (filled circles, e.g., point A) for a given value of R and of I_{tot}. Then, we increase the value of R (this is represented by a horizontal arrow in Fig. 3) at constant total intensity. This drives the system from periodic oscillations into a quasiperiodic beating regime (point B). Then, the small increase of the total intensity at fixed R (this is represented by a vertical arrow) brings the system back into periodic oscillation regime (open triangles, point C). The director precession rate increases with I_{tot} for a fixed value of R, as it is predicted by our theory [Eq. (7)]. The corresponding theoretical fit (solid curve, Fig. 3) gives good quantitative agreement with experimental data. We have used the following material parameters for this curve: $\varepsilon_{\parallel}=2.92$, $\varepsilon_{\perp}=2.28$, $\gamma=0.5$ P, $(K_3-K_1)/K_3=0.379$, $K_3=7.5\times 10^{-7}$ dyne (see e.g., in Ref. [3]). The only adjustable parameter used was the ratio I_{tot}/I_{th} that was found to be quite realistic for our experiment ($I_{tot}/I_{th}=1.0003$).

We have no experimental tools to check predictions of our theory about the twist component of the director reorientation [defined by α in Eq. (8)]. However, these predictions may be qualitatively interpreted in the same manner as in Ref. [8]. Also, we do not have a final interpretation of the problem of beatings and it remains to be clarified. However, a possible explanation may be proposed as follows. It was experimentally and theoretically shown by different groups (B. Zel'dovich, Y. Shen, E. Santamato, etc), that the dynamic modulation of the refractive index (via pure dielectric torque and director reorientation) should introduce a small ''redshift'' of the light frequency. Thus, the single circularly polarized light (in our case) should have a slightly redshifted frequency at the output of the cell. The relative frequency shift between two counterpropagating beams (in our case) will depend upon the coordinate z. For example, this shift is not the same at $z=L$ and $z=L/2$. Thus, instead of an ideal interference pattern, created by two counterpropagating waves (with a *fixed frequency*), we should obtain spatially nonuniform temporal beatings, which could be the origin of the director configuration beatings. When we have a single (i.e., $R=0$) circularly polarized traveling (towards $+z$) beam, then the well-known director regular precession (no beatings) is observed due to the angular momentum transfer from the light to the NLC. Then, we remove a certain fraction of photons from the first input beam and send them in the counterpropagating direction (towards $-z$), i.e., we increase R. This does not stop the director dynamic precession, since the total angular momentum transfer is not yet compensated. That is why the redshift and beatings are observed when we increase R.

The situation is different when two counterpropagating beams have equal intensities ($R=1$). In this case, the transfer of angular momentum of the total light field is compensated and there are no dynamic precessions, and consequently, there is no redshift and no beating. All these regimes ($R=0$, $0<R<1$, and $R=1$) are in very good agreement with our experimental observations.

The director dynamic modulation and light frequency shift are coupled and have comparable characteristic times. The simultaneous change of R and the total intensity could, in principle, be used to tune this coupling, as we did in our experiment. We deal with a complex nonlinear problem; that is why our analytical solution (wave equation) was limited to stationary refractive index modifications (indeed the dn/dt is extremely small). We believe that a rigorous analytical solution should give added insight to this question. This is a fascinating problem and we are currently trying to model it.

IV. SUMMARY

In conclusion, we have shown that one can significantly change the character of the light-induced Freédericksz transition in NLC with a proper choice of the excitation field configuration. This manifests as selective enhancement of certain deformation modes and suppression of others. Complex molecular structures (orientational deformation modes) may thus be created and optically controlled. This includes also the control of the dynamic behavior of these molecular complexes. An example of that is the formation of stable reorientation modes of the FT, induced by the helicoidal standing wave, in contrast to the case of the FT induced by a circularly polarized traveling beam. The dynamic stability in our case is however accompanied by the director twist deformation. The space and time nonlocality of the orientational response of the NLC and the particular self-modulation of the excitation waves play principal roles in these phenomena.

ACKNOWLEDGMENTS

We are grateful to the Natural Sciences and Engineering Research Council of Canada (NSERC) and Fonds pour la Formation de Chercheurs et l'Aide à la Recherche of Quebec (FCAR) for their financial support of this work. We thank P. Balcou and V. Drnoyan for help and discussions. We thank also F. Bretenaker and A. LeFloch for discussions about applications of HSW in laser resonators that gave one of us (T.G.) the idea to apply these waves in NLC.

[1] A. S. Zolot'ko, V. F. Kitaeva, N. Kroo, N. I. Sobolev, and L. Csilag, Pis'ma Zh. Eksp. Teor. Fiz. **32**, 170 (1980) [JETP Lett. **32**, 158 (1980); **34**, 263 (1981) [JETP Lett. **34**, 250 (1981)]; S. D. Durbin, S. M. Arakelian, and Y. R. Shen, Phys. Rev. Lett. **47**, 9 (1981).

[2] N. V. Tabiryan, A. V. Sukhov, and B. Ya. Zel'dovich, Mol. Cryst. Liq. Cryst. **136**, 1 (1986); R. S. Hakopyan, N. V. Tabiryan, and B. Ya. Zel'dovich, Opt. Commun. **46**, 249 (1983).

[3] P. G. de Gennes and J. Prost, *The Physics of Liquid Crystals*, 2nd ed. (Clarendon Press, Oxford, 1993).

[4] L. Marrucci, G. Abbate, S. Ferraiuolo, P. Maddalena, and E. Santamato, Phys. Rev. E **46**, 4859 (1992); E. Santamato, G. Abbate, P. Maddalena, L. Marrucci, and Y. R. Shen, Phys. Rev. Lett. **64**, 1377 (1990).

[5] Traditional normal incidence of the excitation light on a homeotropic NLC cell is considered.

[6] E. Santamato, B. Daino, M. Romangoli, M. Settembre, and Y. R. Shen, Phys. Rev. Lett. **57**, 2423 (1986).

[7] T. V. Galstyan and V. Drnoyan, Phys. Rev. Lett. **78**, 2760 (1997).

[8] See T. V. Galstyan, A. A. Yesayan, and V. Drnoyan, preceding paper, Phys. Rev. E **58**, 4605 (1998), for details of the corresponding theoretical analysis.

[9] V. Evtuhov and A. E. Siegman, Appl. Opt. **4**, 142 (1965).

[10] Corresponding detailed experimental data and theoretical discussion are planned to be presented elsewhere.